Journal of Photochemistry and Photobiology A: Chemistry 332 (2017) 571–579

Contents lists available at ScienceDirect

Journal of Photochemistry and Photobiology A: Chemistry

journal homepage: www.elsevier.com/locate/jphotochem

Transient spectroscopic characterization and theoretical modeling of fulvic acid radicals formed by UV-A radiation

Marcela V. Martin[a], Ricardo A. Mignone[b], Janina A. Rosso[a], Pedro David Gara[c], Reinaldo Pis Diez[d], Claudio D. Borsarelli[b], Daniel O. Mártire[a,*]

[a] Instituto de Investigaciones Fisicoquímicas Teóricas y Aplicadas (INIFTA, CONICET/UNLP), Facultad de Ciencias Exactas, Universidad Nacional de La Plata, Casilla de Correo 16, Sucursal 4, (1900) La Plata, Argentina
[b] Instituto de Bionanotecnología del NOA (INBIONATEC), Universidad Nacional de Santiago del Estero (UNSE); CONICET, RN9, Km 1125, G4206XCP Santiago del Estero, Argentina
[c] Centro de Investigaciones Ópticas (CIOp), CONICET La Plata-CIC, CC 3, (1897) Gonnet, La Plata, Argentina
[d] Centro de Química Inorgánica (CEQUINOR, CONICET/UNLP) Facultad de Ciencias Exactas, Universidad Nacional de La Plata, La Plata, Argentina

ARTICLE INFO

Article history:
Received 16 June 2016
Received in revised form 26 September 2016
Accepted 4 October 2016
Available online 5 October 2016

Keywords:
Fulvic acids
Laser flash photolysis
Photoacoustics
Density functional theory
Phenoxyl radicals
Triplet states

ABSTRACT

Laser flash-photolysis experiments (λ^{exc} = 355 nm) performed with aqueous solutions of Pony Lake and Waskish Peat fulvic acids at pH = 2 showed formation of transient species with absorption maxima at 470–480 nm with O_2-independent lifetimes of 600–700 μs, which were assigned to a phenoxyl radicals. Formation of these radicals occurs after photoionization of the fulvic acids followed by fast deprotonation process. Photoacoustic experiments at the same excitation wavelength yielded the O_2-independent fraction of energy stored at times longer than 135 ns. DFT calculations were performed to estimate the absorption spectra and energy content of the phenoxyl radicals and triplet excited state of the Buffle's model of the fulvic acid. Combination of the DFT and photoacoustic data yielded the photoionization quantum yields of both FA, which were compared to reported values obtained by steady-state and time-resolved techniques.

1. Introduction

The light absorbing fraction of dissolved organic matter is named the chromophoric dissolved organic matter (CDOM), which can originate from both aquatic microbial sources and terrestrial sources such as degraded lignin [1]. The chromophoric properties of CDOM come predominantly from humic substances (HS), which are widely spread materials in soils and waters where they are generated during the microbiological and abiotic degradation of animals and plants [2]. HS are complex, acidic, and amorphous organic polyelectrolytes, which have a yellow to black appearance. Their chemical composition and functional structure are strongly dependent on the geological and environmental conditions existing during their generation. Typically, HS are classified by their aqueous solubility. Humic acids (HA) comprise the fraction of HS only soluble at pH > 2 with average molecular weight between 3 and 5 kDa. Fulvic acids (FA) are soluble under all pH conditions and present lower average molecular weight, *e.g.* <1–2 kDa. Finally, the completely insoluble fraction at all pH is called humin, which is an important component of the soil [3]. Therefore, both HA and FA are the main natural organic macromolecules found in surface waters, where sunlight absorption has important environmental and biological consequences [1].

The UV–visible absorption spectra of HS decreases almost exponentially with the wavelength [4,5], as expected due to the presence of multi-aliphatic and aromatic moieties in the CDOM. Thus, the larger UV absorbing capability of CDOM provides to aquatic organisms a natural UV screening effect from sunlight. Nevertheless, this protection from UV radiation can also induce the formation of excited states species in the CDOM allowing direct and indirect photochemical reactions [6]. In fact, the involvement of triplet excited states of HS, *i.e.* $^3HS^*$ in energy transfer, H-abstraction and electron transfer reactions is well documented [6–8]. Previously, it has been demonstrated the participation of $^3HS^*$ in the photosensitized degradation of organic pollutants in natural waters or in solutions, *e.g.* monuron [8], bisphenol A [9,10], sulfa drugs [11], and 2,4,6-trimethylphenol [12]. Later, Chen et al. [13] investigated the photodegradation of amine drugs in the presence of HS under simulated sunlight. They showed that the $^3HS^*$ were the main reactive species in the photochemical

* Corresponding author.
E-mail address: dmartire@inifta.unlp.edu.ar (D.O. Mártire).

http://dx.doi.org/10.1016/j.jphotochem.2016.10.007
1010-6030/

degradation of the amine drug through an electron-transfer mechanism [13]. Canonica et al. showed that CDOM and aromatic carbonyls, which are well-known photosensitizers, exhibited strong kinetic analogies in their photosensitizing properties toward phenols and phenylurea herbicides [14–17], suggesting that carbonyls groups in HS play a role in photosensitized reactions.

Flash-Photolysis studies performed by Fischer et al. [18] with excitation at 350 nm employing HS from different origin showed transient absorption bands with maximum absorbance at 475 nm and lifetime in the microseconds range and another at 700 nm, attributed to the solvated electron. Power et al. [19] excited at 355 nm Mossy Point (Armdale) FA and identified up to four transient signals at pH = 7. One of them with λ^{max} = 675 nm and lifetime ≈1 μs was assigned to the solvated electron. The second component with λ^{max} = 475 nm and a lifetime of 1–10 μs was assigned to a radical cation on the basis of its concurrent appearance with the solvated electron within 20 ps. The third component with a featureless transient absorption and a lifetime >100 μs was assigned to the triplet states of FA, while the fourth transient absorption signal with a lifetime ≈50 ns remained unidentified. Later, Sul'timova et al. [20] employed the laser excitation at λ^{exc} = 337 nm to investigate the transient species formed upon irradiation of peat FA solutions under alkaline conditions. These authors detected several short-lived intermediates that are efficiently quenched by molecular oxygen, and thus were assigned to triplet states.

In addition, Bruccoleri et al. [21,22] employed magnetic circular dichroism and photoacoustic techniques to determine triplet state energies and quantum yields of Mossy Point (Armdale) and Laurentian FAs in the pH range of 2.5–9.0. The measured triplet energies were in the range from 170 to 190 kJ mol^{-1} with singlet-triplet splitting $\Delta E_{ST} \approx 29$ kJ mol^{-1} and intersystem crossing quantum yields between 0.3 and 0.8.

Considering the complex nature of HS, given by origins and geological processes, exhaustive transient species characterization is needed. In this work, we present a combined laser-flash photolysis and photoacoustic study of FA derived from two classes of precursor organic material [23], *i.e.*, decomposed plant material and soils of terrestrial (allochthonous) origin, *e.g.* Waskish Peat (WPFA); and from organic material produced by algae and bacteria (autochthonous), *e.g.* Pony Lake (PLFA). UV-A pulsed laser at λ^{exc} = 355 nm was used for excitation of the FA solutions at pH < 2, to assure full protonation of the carboxylic acid residuals present in the FA allowing the comparison of the transient absorption spectra with those obtained from theoretical calculations with the protonated Buffle's model [24,25].

Density functional theory (DFT) calculations were carried out on the singlet (ground-state) and excited triplet electronic states of the Buffle's model [26] of fulvic acids, as well as on the phenoxyl radicals that can be formed from it. Their conformational space was examined in a systematic way in the search of lower-energy structures. For the lowest-energy conformations of the triplet electronic state and the phenoxyl radicals the absorption spectra were also calculated to aid in the interpretation of experimental results.

2. Materials and methods

2.1. Materials

Waskish Peat (WPFA) and Pony Lake (PLFA) fulvic acids were from International Humic Substances Society (IHSS) and used as received. The pH of the solutions was adjusted by addition of stock solutions of $HClO_4$ or NaOH, both reagents from Merck. Deionized water (>18 MΩ cm, <20 ppb of organic carbon) was obtained from a Millipore system (Bedford, MA).

2.2. Laser flash photolysis (LFP) experiments

LFP experiments were performed by excitation with the third harmonic of a Nd:YAG Litron laser (2 ns FWHM) at 355 nm. The analysis light from a 150 W Xe arc lamp, was passed through a monochromator (PTI 1695) and detected by a 1P28 PTM photomultiplier. A 10 mm- pathlength cuvette was employed. Decays typically represented the average of 64 pulses and were taken by and stored in a 500 MHz Agilent Infiniium oscilloscope.

2.3. Photoacoustic measurements

Photoacoustic measurements were performed by using a set-up already described [27]. A Q-Switched Nd:YAG laser (7 ns FWHM) operating at 355 nm, was used as excitation source (1 mm diameter in the cell). A home-made ceramic piezoelectric (4 × 4 mm) transducer with an appropriate amplifier was used to detect the acoustic signals. A rectangular slit of 1 mm width was placed in

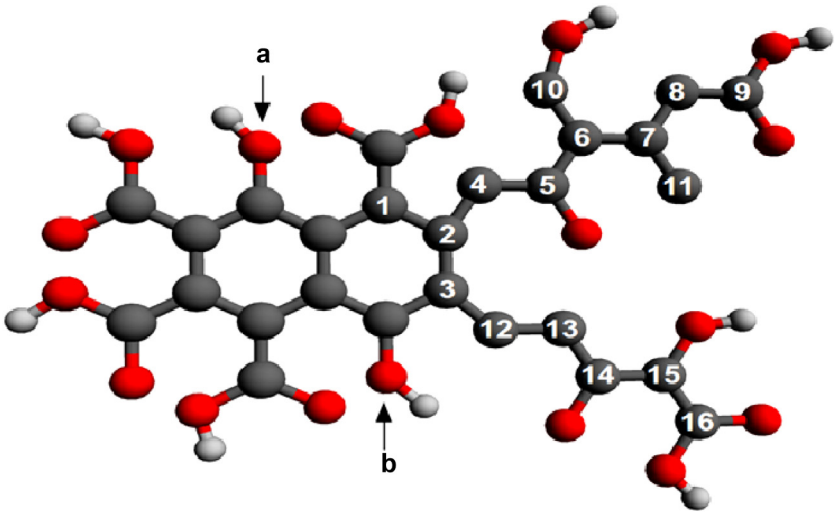

Fig. 1. Schematic drawing of the Buffle's model for fulvic acids. Black, red and white circles represent carbon, oxygen and hydrogen atoms, respectively. Only hydrogen atoms bonded to oxygen atoms are shown. Letters indicate the OH groups involved in the formation of the phenoxyl radical. Selected carbon atoms are numbered to ease the identification of dihedral angles. (For interpretation of the references to colour in this figure legend, the reader is referred to the web version of this article.)

front of the sample holder in order to obtain an acoustic transit time of $\tau_a = 675$ ns. Under this condition, all transient species with lifetimes longer than 135 ns (*i.e.* $\tau_a/5$) can be considered as energy-storing species for the photoacoustic experiment [28]. Measurements were performed by averaging the acoustic signals generated by 64 laser shots for better signal to noise ratio. The laser was operated at a repetition rate of 2 Hz. Comparison of the absorption spectra of the solutions before and after each set of laser shots showed that for all the samples no photobleaching neither photoproducts were observed under the experimental conditions [29]. New Coccine (NC) was used as calorimetric reference [30]. Sample and reference solution concentrations were matched within 2% to absorbance values between 0.08 and 0.22 at the laser excitation wavelength. The experiments were performed either under N_2 or O_2 saturation, bubbling for 20 min with solvent-saturated gas previous to the measurements.

2.4. Fluorescence experiments

Fluorescence spectra were measured with a Hitachi F-2500 (Hitachi High-Technologies Corp., Kyoto, Japan) instrument using excitation and emission slit width of 5 nm. Fluorescence quantum yields (Φ_f) of the HS in aqueous solutions with excitation wavelength at 355 nm were determined by actinometry using as reference quinine sulfate (QS, from Fluka) in 0.5 M H_2SO_4 [31], Eq. (1).

$$\Phi_f{}^S = \Phi_f{}^R \left(\mathrm{Grad}^S/\mathrm{Grad}^R\right)\left(\eta_S{}^2/\eta_R{}^2\right) \quad (1)$$

Where, η_R and η_S are the refractive indices of the sample and reference solutions, respectively. $\Phi_f{}^R = 0.546$ corresponds to the fluorescence quantum yield of QS [31], and $\Phi_f{}^S$ is the fluorescence quantum yield for the sample. Grad^S and Grad^R are the slopes of the plots representing fluorescence integrated area vs absorbance at 355 nm for the sample and reference, respectively (Fig. S1 Supplementary material).

2.5. Computational details

The fulvic acid (FA) was represented by the Buffle's model [32], see Fig. 1. The conformational space of FA was explored using the Self Consistent Charge Density Functional Tight Binding method [33] as implemented in the dftb+ program [34]. The mio-1-1 parameter set was used for the calculations [33]. Several starting structures of FA were generated by selected modifications of dihedral angles of the longer side branches. As low-lying triplet electronic states as well as the phenoxyl radical of FA are also of interest, starting geometries were generated for those states. The OH groups labeled with letters **a** and **b** in Fig. 1 were taken into account to generate the phenoxyl radical. Thus, about 1200 starting structures generated for the four species described were optimized at the SCC-DFTB level of theory and the geometries were analyzed to discard duplicated structures.

The resulting geometries were further optimized using the hybrid GGA exchange-correlation functional PBE0 [35] with the Def2-TZVP basis set for all atoms [36]. To alleviate the computational cost the resolution of the identity in its RIJCOSX version was used [37].

After optimization, the Hessian matrix of the energy with respect to the nuclear coordinates was constructed and diagonalized and its eigenvalues were used to verify whether the geometries are local minima or saddle points on the potential energy surface of the molecules. Only those conformers lying up to 8.4 kJ mol^{-1} above the corresponding ground state were considered for further investigation.

The absorption spectra of the stable conformers of the triplet state and the phenoxyl radical of FA were calculated within the framework of the time-dependent density functional theory [38]. The same density functional and basis sets that were employed for geometry optimization are used to that end.

Solvent effects (water) were considered implicitly through the Conductor-like Screening Model [39] both for geometry optimizations and for the absorption spectra to include electrostatic contributions to the total electronic energy. All the calculations were carried out with the ORCA package [40]. All figures were produced with the aid of the Avogadro program [41].

3. Results and discussion

3.1. Transient species of PLFA and WPFA

Fig. 2 shows the transient absorption spectra of both FA samples observed immediately after the laser pulsed excitation of either both Ar- or O_2-satured solutions. The experimental error bars are the standard deviation for triplicate experiments of the differential transient absorption value (ΔA) after 10 μs of the excitation pulse, obtained by single exponential fitting of the decay curve (inset of Fig. 2). In all cases, the decays fall to $\Delta A\infty = 0$, accordingly with the lack of photobleaching after irradiation. Within the experimental error, both the transient spectra and lifetimes of each species were independent of the presence of O_2, *e.g.* $\tau^{Ar} = 610 \pm 20$ μs and $\tau^{O2} = 600 \pm 20$ μs for PLFA, and $\tau^{Ar} = 690 \pm 20$ μs and $\tau^{O2} = 660 \pm 20$ μs for WPFA. This result suggests that the transient band observed with maximum at ≈480 nm should not be assigned to

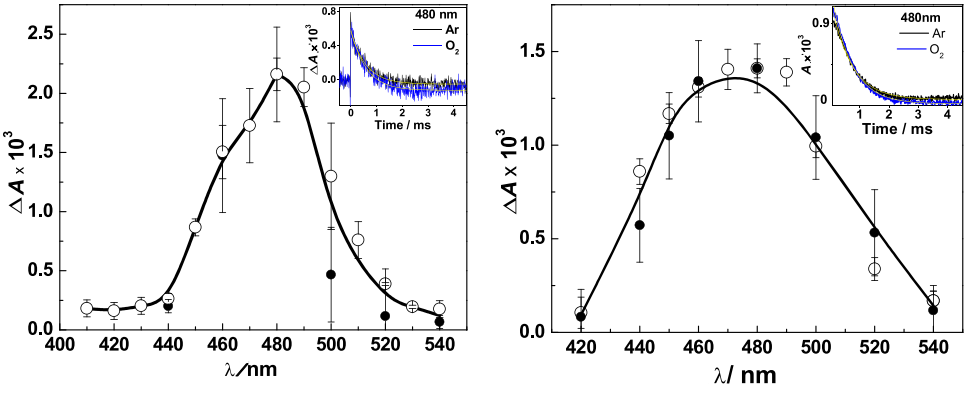

Fig. 2. Transient absorption spectra of the intermediates formed from Ar-saturated (○) and O_2-saturated (•) solutions of Pony Lake (9.8 mg L^{-1}, left) and Waskish Peat (18.8 mg L^{-1}, right) solutions of pH = 2.0 generated in LFP at the excitation wavelength of 355 nm. The insets show the transient decays at 480 nm under Ar and O_2 saturation as indicated.

triplet species, but to radical species of the FA samples as described below.

At the excitation wavelength of our experiments (355 nm) all quinones absorb [42]. The excited states of quinones are better electron acceptors than their ground-states. A plausible explanation of our results includes the postulation of a charge-transfer process from a donor group of FA, such as a polyphenol, to a more oxidized acceptor (A^*) such as a triplet state of a quinone to yield a radical cation of the phenolic moiety ($PhOH^{+}$) and the radical anion of the quinine (A^-) (reaction (2)). In fact, De Laurentiis et al. [43] proposed this mechanism to account for the phototransformation of phenol upon excitation of a quinone sensitizer at 355 nm.

$$PhOH + A^* \rightarrow PhOH^{\bullet+} + A^- \quad (2)$$

$$PhOH^{+} + H_2O \leftrightarrows PhO^{\bullet} + H_3O^{+} \quad (3)$$

However, due to the negative pK_a values of the radical cations of phenols, in the presence of small amounts of water, reaction (3) takes place and the phenoxyl radical is the only observed transient in photosensitized electron transfer processes [44]. Phenoxyl radicals of phenols with electron withdrawing substituents present absorption in the 400–500 nm wavelength range [44,45], in agreement with our data. This mechanism is supported by the physical model proposed for CDOM, in which charge-transfer interactions between electron donating and accepting chromophores within the CDOM control their optical and photophysical properties [1].

The signals intensity at the shortest time measured (10 μs) in the LFP was independent of the concentration of molecular oxygen (Fig. 2). This fact is against the charge-transfer mechanism for the formation of the phenoxyl radicals because in the presence of oxygen the fraction of the precursor triplet states A^* scavenged by PhOH (reaction (2)) should decrease because of the competitive energy transfer from A^* to molecular oxygen to yield singlet oxygen.

A plausible pathway leading to formation of phenoxyl radicals upon 355 nm excitation of CDOM is photoionization (reaction (4)) [46] followed by deprotonation (reaction (3)).

$$PhOH + h\nu \rightarrow PhOH^{+} + e^-_{(aq)} \quad (4)$$

Unfortunately, the low sensitivity of our photomultiplier in the region of 700 nm close to the maximum absorbance of the solvated electron [47] precluded detection of this species. However, the generation of the radical species by reaction (4) is supported by the works of Fischer et al. [18] and Power et al. [19]. These authors observed formation of the solvated electrons and the transient species with absorption maxima at 475 nm.

In order to further corroborate whether the photoionization route is the responsible for the formation of the phenoxyl radicals, photoacoustic measurements were done to determine the fraction of energy released to the medium as prompt heat in N_2- and O_2-saturated solutions.

3.2. Photoacoustic measurements

Fig. 3 shows the laser energy-normalized photoacoustic signals for the reference NC (solid line), and the sample PLFA in N_2- (dotted line) and O_2- (dashed line) saturated aqueous solutions of the same absorbance at 355 nm.

In all cases, the photoacoustic signals of both FA samples were in phase with that of the calorimetric reference NC. As it has been well discussed [31,48,49], this type of photoacoustic behavior corresponds to a relaxation process of the excited states much faster that the integration time of the piezoelectric transducer, *e.g.* $\tau_a/5 \approx 135$ ns, where τ_a is the transit acoustic time of the experiment (675 ns). Under this condition, all transient species with lifetimes longer than 135 ns can be considered as energy-storing species for the photoacoustic experiment [28].

In the case of the acoustic signal for NC, a dye without photochemistry and formation of long-lived excited species [30], all the deactivation processes take place in a time $<<\tau_a/5$ by non-radiative relaxation and it can be considered as 100% of prompt heat released to the solution without volume contribution to the acoustic signal [48]. Then, the acoustic signal of the sample accounts for the prompt formation of long-lived storing-energy species such as the phenoxyl radical of the FA ($\tau \sim 650$ μs) (see LFP experiments). In this case, the peak to peak amplitude of the first acoustic pulse (H) was used to measure the prompt heat (α) released to the medium by the sample within the time resolution of the experiment (Amplitude method) [50]. Plots of H as a function of the excitation fluence (F) for the reference NC and for the FA samples in the presence of N_2 or O_2, show linear relationships and excellent reproducibility at different absorbances for laser fluences lower than 30 J m^{-2}. These results can be interpreted by using Eq. (5) [49],

$$\frac{H}{F} = K\alpha\left(1 - 10^{-A_{355}}\right) \quad (5)$$

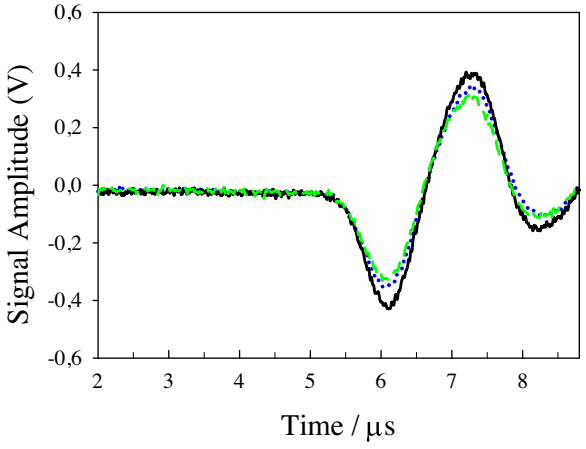

Fig. 3. Photoacoustic signals of New coccine (NC, solid line: Air) and PLFA (dashed line: saturated in O_2, dotted line: in N_2) measured in water solutions of matched absorbance (0.105 ± 0.001) at 25 °C.

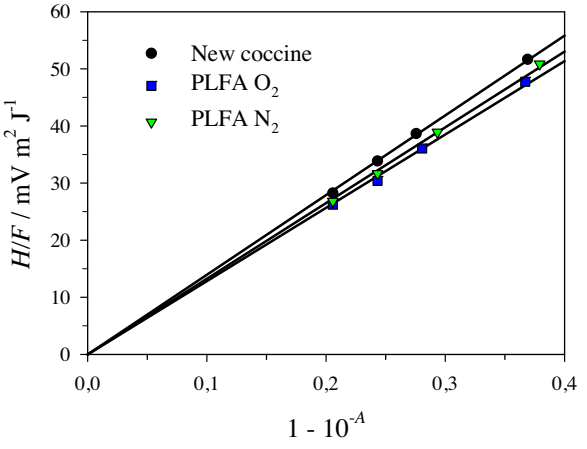

Fig. 4. Amplitude of the fluence-normalized photoacoustic signals as a function of the fraction of absorbed energy for aqueous solutions of PLFA in O_2 (squares), N_2 (triangles) and NC (circles).

Table 1
Photophysical data of fulvic acids in aqueous solutions, determined in this work.

Humic Substance		$E_\lambda = \alpha E_\lambda + E_f\Phi_f + E_{st}\Phi_{st}$					
		$\alpha_{FA} \pm 0.09$	αE_λ [(a)] (kJ mol^{-1})	$E_f\Phi_f$ [(b)] (kJ mol^{-1})	$E_{st}\Phi_{st}$ [(c)] (kJ mol^{-1})	$\Phi_{st} \pm 0.02$	Φ_{st} [LL(d)]
PLFA	pH 2 / N_2	0.94	317	3.30	16.94	0.06	0.05
PLFA	pH 2 / O_2	0.92	312	2.93	22.47	0.08	0.07
WPFA	pH 2 / N_2	0.94	316	1.43	19.42	0.07	0.06
WPFA	pH 2 / O_2	0.94	317	1.34	18.90	0.07	0.06

Experimental errors: (a) ±10%, (b) ±5%, (c) ±15%. (d) Lower limit of Φ_{st} obtained taking E_{st} = 337 kJ mol^{-1}.

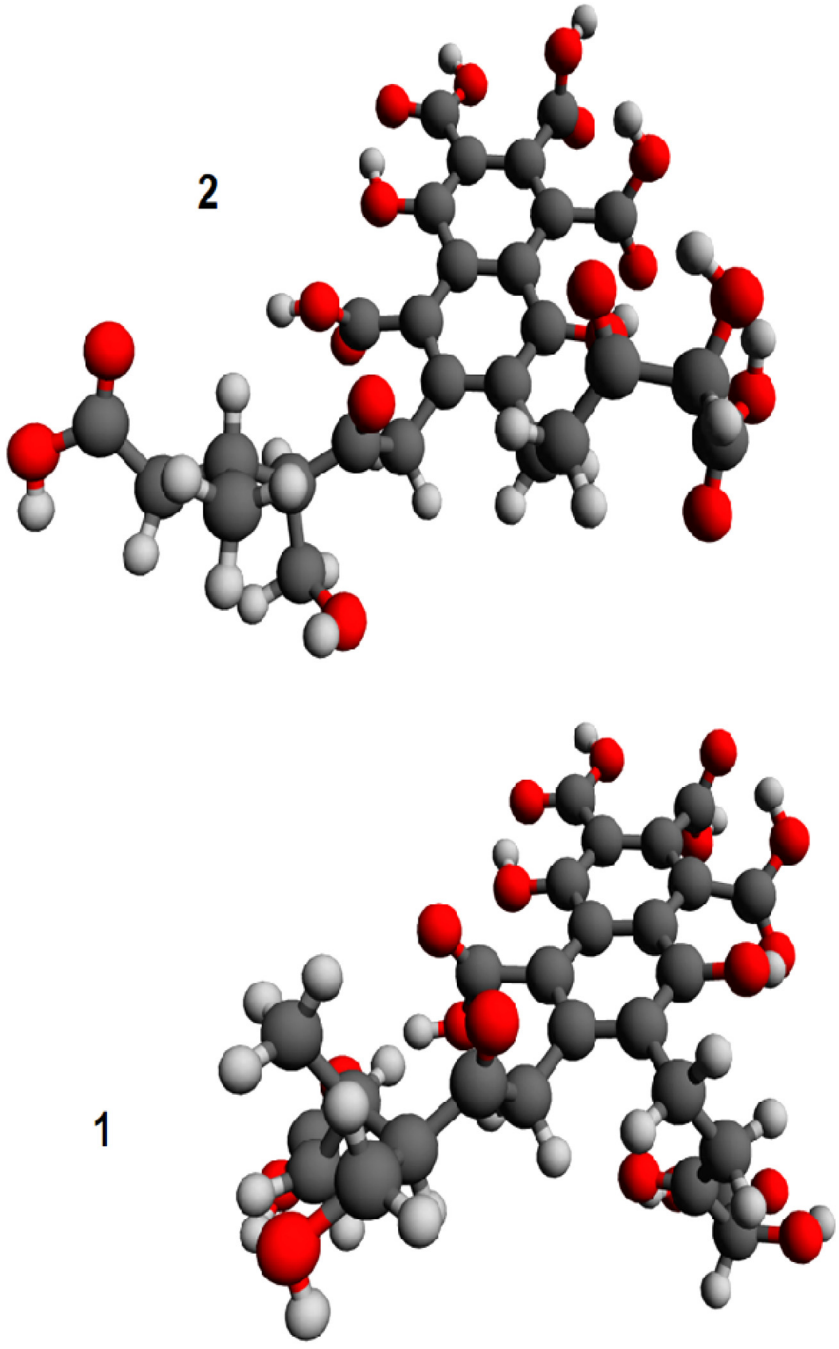

Fig. 5. Stable conformations of the Buffle's model for fulvic acids in its singlet electronic state. Black, red and white circles represent carbon, oxygen and hydrogen atoms, respectively. Conformer **2** is 5.06 kJ mol^{-1} higher in energy than conformer **1**. (For interpretation of the references to colour in this figure legend, the reader is referred to the web version of this article.)

where K is an experimental constant containing the thermoelastic properties of the solution and instrumental factors, A_{355} is the sample absorbance at the excitation wavelength (355 nm), and α is the fraction of energy released to the medium as prompt heat. Fig. 4 shows linear plots of H/F as a function of the fraction of absorbed energy for reference and PLFA in solutions with O_2 and with A_{355} between 0.08 and 0.22. The H/F values for each solution were obtained from the corresponding linear plots of H *vs* F.

Taking into account that $\alpha_{NC} = 1$ for NC and that the measurements for sample and reference were performed under the same experimental conditions, the slope ratio between the plots of Fig. 4 for FA and NC yielded the $_{\alpha FA}$ values of FA (Table 1). Hence, the energy balance is given by Eq. (6),

$$E_\lambda = \alpha_{FA} E_\lambda + \Phi_f E_f + \Phi_{st} E_{st} \quad (6)$$

where; E_λ is the energy of the excitation laser ($\equiv$337 kJ mol^{-1}); E_f is the energy level of the lowest singlet excited state and Φ_f is the fluorescence quantum yield in N_2-saturated solutions; while Φ_{st} and E_{st} are the formation quantum yield and the energy content of the long-lived state, respectively. The E_f value for each FA was estimated by overlapping energy between the normalized excitation and emission spectra of the FA (Fig. S2 Supplementary material).

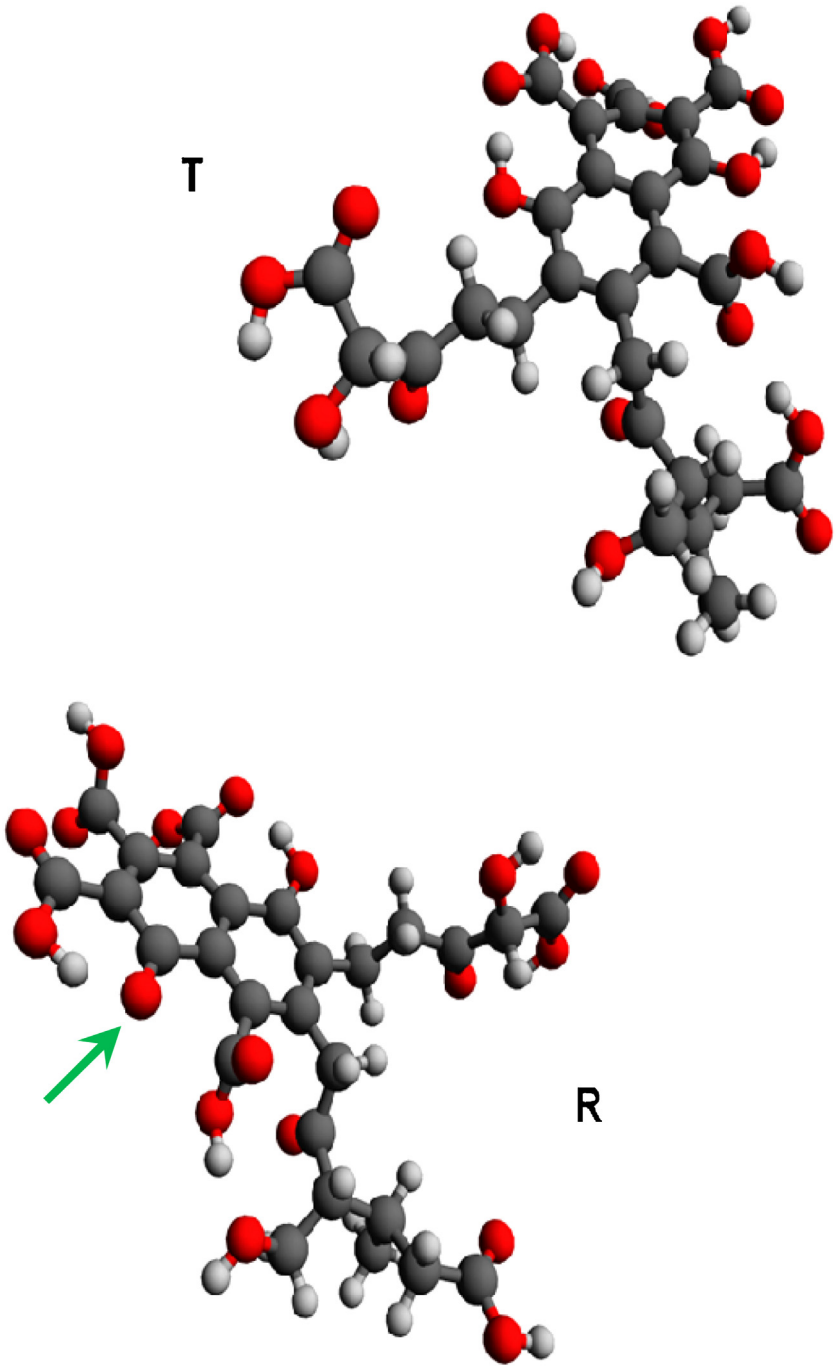

Fig. 6. Stable conformations of the Buffle's model for fulvic acids in its triplet electronic state (**T**) and as phenoxyl radical (**R**). Black, red and white circles represent carbon, oxygen and hydrogen atoms, respectively. The arrow indicates the location of the H atom removed for the generation of the phenoxyl radical. (For interpretation of the references to colour in this figure legend, the reader is referred to the web version of this article.)

The independence of the α_{FA} values of the concentration of molecular oxygen further supports the assignment of the transient to the phenoxyl radical of FA.

3.3. Theoretical calculations

In order make sure whether it is reasonable that the species observed in the LFP experiments is a phenoxyl radical formed by reactions (4) and (3), DFT theoretical calculations of the absorption spectra and energy content of the triplet state and phenoxyl radicals of the Buffle's model were performed. For completeness, the singlet ground state corresponding to the Buffle's model was also investigated.

Results of the conformational search on the ground state singlet electronic state of the Buffle's model in the solvent phase (water) show two stable conformations (**1** and **2**) within the threshold of 8.4 kJ mol^{-1}. Conformer **2** is only 5.1 kJ mol^{-1} above conformer **1**. The most important differences between the two conformations lie in the shorter side branch, see Fig. 5 and Table S1 in the Supplementary material, which shows some selected dihedral angles.

In the case of the triplet electronic state of the Buffle's model in water, one conformation is favored with respect to the others in more than 25 kJ mol^{-1}, thus that conformation, **T** from now on, is considered for further investigation, see Fig. 6. Selected geometrical parameters of the most stable triplet state are shown in Table S1. It can be seen from the table that the triplet electronic state undergoes appreciable conformational changes when it is formed from the singlet electronic state of the Buffle's model.

Conformer **T** is found to be 150.7 kJ mol^{-1} higher in energy than conformer **1**, whereas it is 145.6 kJ mol^{-1} above conformer **2**. These values are in very good agreement with data obtained for FA from photoacoustic experiments and magnetic circular dichroism spectra, which are in the range 170–190 kJ mol^{-1} [21,22].

The phenoxyl radical is formed allowing the removal of H-atom from the OH groups labeled **a** and **b** in Fig. 1. Interestingly, a conformer obtained by removing the H-atom from the **a** site becomes the more stable phenoxyl radical found in the present work, it will be called **R** from now on. Another stable phenoxyl radical obtained from site **a** is found to be about 29 kJ mol^{-1} above conformer **R**. On the other hand, the most stable phenoxyl radical obtained from site **b** is more than 50 kJ mol^{-1} higher in energy than conformer **R**. Selected geometrical parameters of the most stable phenoxyl radical, **R**, are listed in Table S1 and Fig. 6 shows its optimized structure. Further studies are carried out on that conformation.

On the other hand, addition of reactions (4) and (3) (photoionization followed by deprotonation of the radical cation) yield reaction (7).

$$\text{R-OH} + \text{H}_2\text{O} + h\nu \rightarrow \text{R-O}^{\bullet} + \text{H}_3\text{O}^{+} + \text{e}^{-}_{(aq)} \quad (7)$$

The reaction energies for the above equation were calculated for the conversion of conformers **1** and **2** into the phenoxyl radical **R**. The reaction energies are 278.3 and 272.7 kJ mol^{-1} when R-OH is conformer **1** and conformer **2**, respectively. For the calculation it was assumed that the thermal corrections to convert the total electronic energy to Gibbs free energy cancel when the R-OH + H_2O contribution is subtracted from the R-O$^{\bullet}$ + H_3O^{+} contribution. For the Gibbs free energy of the solvated electron the experimental value of −307 kJ mol^{-1} is considered [51]. The above reaction energies correspond to wavelengths of 430 and 438 nm, respectively, which suggest that the phenoxyl radical could be formed by irradiating the singlet electronic states of the Buffle's model with light of 355 nm.

Absorption spectra are calculated for conformers **T** and **R** (Fig. 7). From the comparison of Figs. 2 and 7, it can be seen that there is good agreement between experimental and calculated spectra. The shape of the calculated spectra is very similar to experimental ones. It is also evident from the figure that calculated spectra are blue-shifted by about 100 nm. The absorption maxima of conformers **T** and **R** are found at about 320 and 350 nm, respectively. Despite the shift to low wavelengths, the theoretical results clearly suggest that both the triplet electronic state and the phenoxyl radical could account for the experimental transient spectra shown in Fig. 2. However, experimental LFP and photoacoustic data support the assignment to the phenoxyl radical.

3.4. Calculation of the quantum yield of reaction (7)

The good agreement between the triplet energy content calculated here for the Buffle's model and reported photoacoustic data [21,22] encouraged us to calculate the quantum yield of

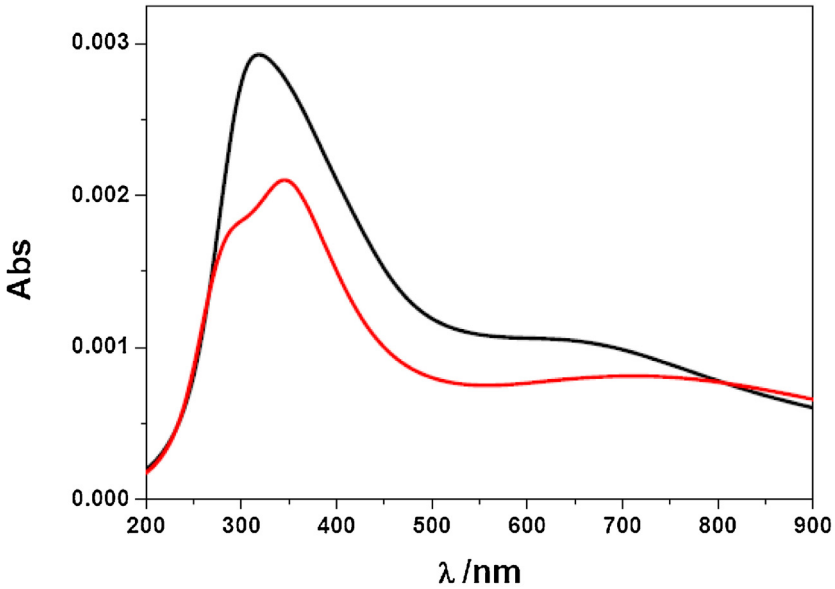

Fig. 7. Simulated spectra for conformers of the Buffle's model for fulvic acids in its triplet electronic state **T** (black) and as phenoxyl radical **R** (red). (For interpretation of the references to colour in this figure legend, the reader is referred to the web version of this article.)

reaction (7) from the values of $E_{st}\Phi_{st}$ measured here for the FA and our theoretical value of energy content of reaction (7) as E_{st}. Considering conformers **1** and **2** and the phenoxyl radical **R**, E_{st} = 278.3 kJ mol^{-1}, and the values of Φ_{st} listed in Table 1 are obtained. These photoionization quantum yields are on the order of those obtained for FA and CDOM by LFP [21,52]. However, it is now accepted from steady-state measurements that the photoionization quantum yields of humic substances vary from approximately 10^{-5} to 10^{-4} over the wavelength range 300–400 nm [53]. To account for this discrepancy, it was argued that the higher values obtained in LFP experiments are due to multiphoton ionization [52].

It could be possible that when high laser fluences are employed, multiphoton excitation occurs in LFP experiments. However, this is not the case of the photoacoustic experiments, where <100 μJ per pulse after the rectangular slit was measured. Under these conditions the linear plots shown in Fig. 4 guarantees the single-photon conditions for the photoacoustic experiments. Considering the upper limit for E_{st}, which is the excitation energy of 337 kJ mol^{-1}, the calculated lower limit for Φ_{st}, *i.e.* Φ_{st}^{LL}, is obtained (Table 1). These values are almost coincident with those obtained when the calculated energy of reaction (7) is employed (compare the last two columns of the table). All these results seem to indicate that multiphotonic irradiation is not the reason for the discrepancy between the steady-state and time-resolved photoionization quantum yields of humic substances or CDOM.

4. Conclusion

We present here experimental and theoretical evidence for the formation of phenoxyl radicals of fulvic acids upon irradiation in the UV-A region. The generation of this type of radicals was previously shown by EPR measurements with humic acids solutions exposed to UV and visible light [54]. Formation of CDOM phenoxyl radicals was also inferred from accelerated sensitized photolysis observed when probe compound concentrations decrease below approximately 1 μM [1].

Given the low efficiencies of formation in natural waters and the fact that other components such as tryptophan (free or in combined form) generate solvated electrons upon irradiation, it is unlikely that CDOM-derived e^-_{aq} has a significant environmental impact [52]. However, phenoxyl radicals can be formed not only upon photoionization, but also as a result of charge-transfer processes (see reactions (4) and (3)). Although the importance of charge-transfer interactions in the photophysics and photochemistry of CDOM is recognized [1], the role of the phenoxyl radicals as photooxidants able to react with a huge variety of compounds [55] in the degradation of contaminants in natural waters is disregarded.

Acknowledgements

M.V.M. thanks Consejo Nacional de Investigaciones Científicas y Técnicas (CONICET, Argentina) for fellowships. R.A.M., J.A.R., R.P.D., and C.D.B. are research members of CONICET. P.D.G. and D.O.M. are research members of Comisión de Investigaciones Científicas de la Provincia de Buenos Aires (CIC, Argentina). Authors would like to thank the financial support of the following Argentinean Institutions: Universidad Nacional de Santiago del Estero, Universidad Nacional de La Plata, CONICET (PIO-UNSE-2014-12CO) and FONCyT (PICT-2015-0828; PICT 2012-2359).

Appendix A. Supplementary data

Supplementary data associated with this article can be found, in the online version, at http://dx.doi.org/10.1016/j.jphotochem.2016.10.007.

References

[1] C.M. Sharpless, N.V. Blough, The importance of charge-transfer interactions in determining chromophoric dissolved organic matter (CDOM) optical and photochemical properties, Environ. Sci.: Processes Impacts 16 (2014) 654–671.
[2] G. Davies, E.A. Ghabbour, Humic substances, Structure, Properties and Uses, Royal Society of Chemistry (RSC), Cambridge, UK, 1998.
[3] E.M. Thurman, Organic Geochemistry of Natural Waters, Martinus Nijhoff/Junk, Netherlands, 1985.
[4] M. Domeizel, A. Khalil, P. Prudent, UV spectroscopy: a tool for monitoring humidification and proposing an index of the maturity of compost, Bioresour. Technol. 94 (2004) 177–184.
[5] R.A. Mignone, M.V. Martin, F.E.M. Vieyra, V.I. Palazzi, B.L. de Mishima, D.O. Martire, C.D. Borsarelli, Modulation of optical properties of dissolved humic substances by their molecular complexity, Photochem. Photobiol. 88 (2012) 792–800.
[6] R.G. Zepp, P.F. Schlotzhauer, R.M. Sink, Photosensitized transformations involving electronic energy transfer in natural waters: role of humic substances, Environ. Sci. Technol. 19 (1985) 74–81.
[7] J.-P. Aguer, D. Tétégan, C. Richard, Humic substances mediated phototransformation of 2,4,6-trimethylphenol: a catalytic reaction, Photochem. Photobiol. Sci. 4 (2005) 451–453.
[8] D. Vialaton, C. Richard, J.-P. Aguer, F. Andreux, Transformation of monuron photosensitized by soil-extracted humic substances: energy or hydrogen atom transfer, J. Photochem. Photobiol. A 111 (1997) 265–271.
[9] M. Zhan, X. Yang, Q. Xian, L. Kong, Photosensitized degradation of bisphenol A involving reactive oxygen species in the presence of humic substances, Chemosphere 63 (2006) 378–386.
[10] Y.P. Chin, P.L. Miller, L. Zeng, K. Cawley, L.K. Weavers, Photosensitized degradation of bisphenol A by dissolved organic matter, Environ. Sci. Technol. 38 (2004) 5888–5894.
[11] A.L. Boreen, W.A. Arnold, K. McNeill, Triplet-sensitized photodegradation of sulfa drugs containing six-membered heterocyclic groups: identification of an SO_2 extrusion photoproduct, Environ. Sci. Technol. 39 (2005) 3630–3638.
[12] S. Halladja, A. ter Halle, J.-P. Aguer, A. Boulkamh, C. Richard, Inhibition of humic substances mediated photooxygenation of furfuryl alcohol by 2,4,6-trimethylphenol. Evidence for reactivity of the phenol with humic triplet excited states, Environ. Sci. Technol. 41 (17) (2007) 6066–6073.
[13] Y. Chen, C. Hu, X.J. Qu, Indirect photodegradation of amine drugs in aqueous solution under simulated sunlight, Environ. Sci. Technol. 43 (2009) 2760–2765.
[14] S. Canonica, U. Jans, K. Stemmler, J. Hoigné, Transformation kinetics of phenols in water: photosensitization by dissolved natural organic material and aromatic ketones, Environ. Sci. Technol. 29 (1995) 1822–1831.
[15] S. Canonica, B. Hellrung, P. Müller, J. Wirz, Aqueous oxidation of phenylurea herbicides by triplet aromatic ketones, Environ. Sci. Technol. 40 (2006) 6636–6641.
[16] S. Canonica, Oxidation of aquatic organic contaminants induced by excited triplet states, CHIMIA 61 (2007) 641–644.
[17] A.C. Gerecke, S. Canonica, S.R. Müller, M. Schärer, R.P. Schwarzenbach, Quantification of dissolved natural organic matter (DOM) mediated phototransformation of phenylurea herbicides in lakes, Environ. Sci. Technol. 35 (2001) 3915–3923.
[18] A.M. Fischer, J.S. Winterle, T. Mill, Photochemistry of environmental aquatic systems, chapter 11, ACS Symposium Series, Washington: American Chemical Society, 1987.
[19] J. Power, C.H. Langford, D. Sharma, R. Bonneau, Laser flash photolytic studies of a well-characterized soil humic substance, ACS-Symp. Ser. No. 327 (1987) 158–173.
[20] N.B. Sul'timova, P.P. Levin, O.N. Chaikovskaya, I.V. Sokolova, Laser photolysis study of the triplet states of fulvic acids in aqueous solutions, High Energy Chem. 42 (2008) 464–468.
[21] A. Bruccoleri, C.H. Langford, C. Arbour, Pulsed photo acoustic evaluation of intersystem crossing quantum yields in fulvic acid, Environ. Technol. (1990) 169–172.
[22] A. Bruccoleri, B.C. Pant, D.K. Sharma, C.H. Langford, Evaluation of primary photoproduct quantum yields in fulvic acid, Environ. Sci. Technol. 27 (1993) 889–894.
[23] D.M. McKnight, G.R. Aiken, Sources and age of aquatic humus, in: D. Hessen, L. Tranvik (Eds.), Aquatic Humic Substances, Springer-Verlag, Berlin, 1998 (pp. 39).
[24] P. Saparpakorn, J.H. Kim, S. Hannongbua, Investigation on the binding of polycyclic aromatic hydrocarbons with soil organic matter: a theoretical approach, Molecules 12 (2007) 703–715.
[25] P.M. David Gara, G.N. Bosio, M.C. Gonzalez, N. Russo, M. del, C. Michelini, R. Pis Diez, D.O. Mártire, A combined theoretical and experimental study on the oxidation of fulvic acid by the sulfate radical anion, Photochem. Photobiol. Sci. 8 (2009) 992–997.

[26] J. Buffle, F.L. Greter, W. Haerdi, Measurement of complexation properties of humic and fulvic acids in natural waters with lead and copper ion-selective electrodes, Anal. Chem. 49 (1977) 216–222.
[27] H.H. Martinez Saavedra, F. Ragone, G.T. Ruiz, P.M. David Gara, E. Wolcan, Solvent dependent switching of ^{3}MLLCT and ^{1}IL luminescent states in [ClRe(CO)^{3}(Bathocuproinedisulfonate)]$^{2-}$: spectroscopic and computational study, J. Phys. Chem. A 118 (2014) 9661–9674.
[28] S.E. Braslavsky, G.E. Heibel, Time-resolved photothermal and photoacoustic methods applied to photoinduced processes in solution, Chem. Rev. 92 (1992) 1381–1410.
[29] G.N. Bosio, P. David Gara, F.S. García Einschlag, M.C. González, M.T. del Panno, D.O. Mártire, Photodegradation of soil organic matter and its effect on gram (−) bacterial growth, Photochem. Photobiol. 84 (2008) 1126–1132.
[30] S. Abbruzzetti, C. Viappiani, D.H. Murgida, R. Erra-Balsells, G.M. Bilmes, Non-toxic, water-soluble photocalorimetric reference compounds for UV and visible excitation, Chem. Phys. Lett. 304 (1999) 167–172.
[31] W.H. Melhuish, Quantum efficiencies of fluorescence of organic substances: effect of solvent and concentration of the fluorescent solute, J. Phys. Chem. 65 (2) (1961) 229–235.
[32] J. Buffle, Les substances humiques et leurs interactions avec les ions mineraux, Conference Proceedings de la Commission d'Hydrologie Appliquee de A.G.H.T. M, l'Universite d'Orsay, 1977, pp. 3–10.
[33] M. Elstner, D. Porezag, G. Jungnickel, J. Elsner, M. Haugk, T. Frauenheim, S. Suhai, G. Seifert, Self-consistent-charge density-functional tight-binding method for simulations of complex materials properties, Phys. Rev. B 58 (1998) 7260.
[34] B. Aradi, B. Hourahine, Th. Frauenheim, DFTB+, a sparse matrix-based implementation of the DFTB method, J. Phys. Chem. A 111 (2007) 5678–5684.
[35] C. Adamo, V. Barone, Toward reliable density functional methods without adjustable parameters: the PBE0 model, J. Chem. Phys. 110 (1999) 6158–6170.
[36] F. Weigend, R. Ahlrichs, Balanced basis sets of split valence, triple zeta valence and quadruple zeta valence quality for H to Rn: design and assessment of accuracy, Phys. Chem. Chem. Phys. 7 (2005) 3297–3305.
[37] F. Neese, F. Wennmohs, A. Hansen, U. Becker, Efficient, approximate and parallel Hartree-Fock and hybrid DFT calculations. A 'chain-of-spheres' algorithm for the Hartree-Fock exchange, Chem. Phys. 356 (2009) 98–109.
[38] T. Petrenko, S. Kossmann, F. Neese, Efficient time-dependent density functional theory approximations for hybrid density functionals: analytical gradients and parallelization, J. Chem. Phys. 134 (2011) 054116.
[39] S. Sinnecker, A. Rajendran, A. Klamt, M. Diedenhofen, F. Neese, Calculation of solvent shifts on electronic g-Tensors with the conductor-like screening model (COSMO) and its self-consistent generalization to real solvents (Direct COSMO-RS), J. Phys. Chem. A 110 (2006) 2235–2245.
[40] F. Neese, The ORCA program system, Wiley Interdiscip. Rev.: Comput. Mol. Sci. 2 (2012) 73–78.
[41] Avogadro: an open-source molecular builder and visualization tool. Version 1.2.0. http://avogadro.openmolecules.net/.
[42] R.H. Thomson, Naturally Occurring Quinones, second edition, Academic Press, London, 1971.
[43] E. De Laurentiis, V. Maurino, C. Minero, D. Vione, G. Mailhot, M. Brigante, Could triplet-sensitised transformation of phenolic compounds represent a source of fulvic-like substances in natural waters, Chemosphere 90 (2013) 881–884.
[44] T.A. Gadosy, D. Shukla, L.J. Johnston, Generation, characterization, and deprotonation of phenol radical cations, J. Phys. Chem. A 103 (1999) 8834–8839.
[45] P. Caregnato, P.M. David Gara, G.N. Bosio, M.C. Gonzalez, N. Russo, M. del, C. Michelini, D.O. Mártire, Theoretical and experimental investigation on the oxidation of gallic acid by sulfate radical anions, J. Phys. Chem. A 112 (2008) 1188–1194.
[46] R.G. Zepp, A.M. Braun, J. Hoigné, J.A. Leenheer, Photoproduction of hydrated electrons from natural organic solutes in aquatic environments, Environ. Sci. Technol. 21 (1987) 485–490.
[47] R.M. Musat, A.R. Cook, J.P. Renault, R.A. Crowell, Nanosecond pulse radiolysis of nanoconfined water, J. Phys. Chem. C 116 (2012) 13104–13110.
[48] T. Gensch, C. Viappiani, Time-resolved photothermal methods: accessing time-resolved thermodynamics of photoinduced processes in chemistry and biology, Photochem. Photobiol. Sci. 2 (7) (2003) 699–721.
[49] L.J. Rothberg, J.D. Simon, M. Bernstein, K.S. Peters, Pulsed laser photoacoustic calorimetry of metastable species, J. Am. Chem. Soc. 105 (1983) 3464–3468.
[50] C. Martí, O. Jürgens, O. Cuenca, M. Casals, S. Nonell, Aromatic ketones as standards for singlet molecular oxygen $O_2(1\triangle g)$ photosensitization. Time-resolved photoacoustic and near-IR emission studies, J. Photochem. Photobiol. A 97 (1996) 11–18.
[51] C.D. Borsarelli, S.G. Bertolotti, C.M. Previtali, Thermodynamic changes associated with the formation of the hydrated electron after photoionization of inorganic anions: a time-resolved photoacoustic study, Photochem. Photobiol. Sci. 2 (2003) 791–795.
[52] W. Wang, O.C. Zafiriou, I.-Y. Chan, R.G. Zepp, N.V. Blough, Production of hydrated electrons from photoionization of dissolved organic matter in natural waters, Environ. Sci. Technol. 41 (2007) 1601–1607.
[53] T.E. Thomas-Smith, N.V. Blough, Photoproduction of hydrated electron from constituents of natural waters, Environ. Sci. Technol. 35 (2001) 2721–2726.
[54] K. Polewski, D. Sławińska, J. Sławiński, A. Pawlak, The effect of UV and visible light radiation on natural humic acid: EPR spectral and kinetic studies, Geoderma 126 (2005) 291–299.
[55] P. Neta, J. Grodkowski, Rate constants for reactions of phenoxyl radicals in solution, Phys. Chem. Ref. Data 34 (2005) 109–199.